
Article:
Alonso-Rangel, L., Benítez-Guerrero, T., Martínez-Vieyra, I. et al. (4 more authors) (2017) A role for dystroglycan in the pathophysiology of acute leukemic cells. Life Sciences, 182. pp. 1-9. ISSN 0024-3205

https://doi.org/10.1016/j.lfs.2017.06.004

A role for dystroglycan in the pathophysiology of acute leukemic cells

Lea Alonso-Rangel[a], Tizziani Benítez-Guerrero[a], Ivette Martínez-Vieyra[a], Bulmaro Cisneros[b], Adolfo Martínez-Tovar[c], Steve J. Winder[d] and Doris Cerecedo[a*]

[a]Laboratorio de Hematobiología, Escuela Nacional de Medicina y Homeopatía (ENMH), Instituto Politécnico Nacional (IPN), Mexico City, Mexico
[b]Departamento de Genética y Biología Molecular, Centro de Investigación y de Estudios Avanzados del IPN (Cinvestav-IPN), Mexico City, Mexico
[c]Servicio de Hematología, Hospital General de México Dr. Eduardo Liceaga, Mexico City, Mexico
[d]Department of Biomedical Science, University of Sheffield, Sheffield, UK

*Correspondence: Dra. Doris A. Cerecedo Mercado, Laboratorio de Hematobiología, Escuela Nacional de Medicina y Homeopatía, IPN, Guillermo Massieu Helguera no. 239, Col. La Escalera Ticomán, 07320 Ciudad de México (CDMX),, México. Phone: (+52) (55) 5729 6300, ext. 55531; Fax: (+52) (55) 5729 6300, ext. 55532; E-mail: dcereced@prodigy.net.mx

Key words: Kasumi-1 cells; HL-60 cells; differentiation; phagocytosis; macrophage-like cells.

Abstract

Aims: Previous reports have demonstrated that alterations or reduced expression of Dystroglycan (Dg) complex (αDg and βDg subunits) are related to progression and severity of neoplastic solid tissues. Therefore we determined the expression pattern and subcellular distribution of Dg complex in Acute Myeloid Leukemia (AML) primary blasts (M1, M2, and M3 phenotypes), as well as HL-60 and Kasumi-1 leukemia cell lines. Additionally, we evaluated the relative expression of the main enzymes controlling α-Dg glycosylation to ascertain the post-translational modifications in the leukemia cell phenotype.

Main methods: Primary leukemia blasts and leukemia cell lines were processed by confocal analysis to determine the subcellular distribution of α-Dg, β-Dg, and phosphorylated β-Dg (Y892), to evaluate the expression pattern of the different Dg species we performed Western Blot (WB) assays, while the messenger RNA (mRNA) expression of enzymes involved in α-Dg glycosylation, such as POMGnT1, POMT1, POMT2, LARGE, FKTN, and FKRP, were evaluated by qualitative Reverse Transcription-Polymerase Chain Reaction (qRT-PCR). Finally, in an attempt to ameliorate the leukemia cell phenotype, we transfected leukemia cells with a plasmid expressing the Dg complex.

Key findings: The Dg complex was altered in leukemia cells, including decreased mRNA, protein, and α-Dg glycosylated levels, mislocalization of β-Dg, and a diminution of mRNA expression of LARGE in patients leukemia blasts and in cell lines. Interestingly, the exogenous expression of Dg complex promoted filopodial formation, differentiation, and diminished proliferation, attenuating some HL-60 and Kasumi cells characteristics.

Significance: Dg complex integrity and balance are required for a proper hematopoietic cell function, in that its disruption might contribute to leukemia pathophysiology.

1. Introduction

Dystroglycan (Dg) is encoded by the *DAG1* gene, generating a polypeptide precursor of 895 amino acids, which undergoes post-translational proteolytic cleavage, resulting in two noncovalently associated subunits α and β [1, 2]. α-Dg plays important roles in the deposition, organization, and stability of basement membranes [3], while β-Dg is a transmembrane protein with its cytoplasmic tail bound to utrophin or dystrophin, two spectrin-like molecules that interact with a number of proteins, including F-actin [4].

The physiological role of Dg is to establish communication between cells and their microenvironment, making connections with the extracellular matrix proteins and cytoskeletal elements. The following three different types of glycan modifications extensively decorate α-Dg: mucin-type O-glycosylation; O-mannosylation, and N-glycosylation. The state of α-Dg glycosylation has shown to be critical for the ability of the protein to bind to laminin globular domain-containing proteins of the ExtraCellular Matrix (ECM) [5]. Laminins are part of several proteins that comprise the ECM and that modulate functions such as cell proliferation, adhesion, migration, differentiation, cell polarity, responsiveness to soluble factors, and angiogenesis [6, 7]. β-Dg also participates in cell signalling through a scaffolding role for the ERK/MAPKinase pathway, and by signalling through the phosphorylation of tyrosine 892 of β-Dg by Src, regulating the interaction between Dg and dystrophin, utrophin and other cytoskeletal binding partners [8, 9].

The interaction of Dg with laminin depends on O-linked carbohydrate modifications of the α-Dg mucin domain that, in turn, depend on a large number of glycosylation pathway enzymes involved in α-Dg modification [10]. Defects of Dg glycosylation caused by a loss of function of this protein as an ECM receptor manifest in a wide spectrum of muscular and brain abnormalities [11, 12] as well as in cancer cell lines [13-15].

Changes in α-Dg glycosylation may also play a role in cancer progression [16, 17], which may have an important anti-tumorigenic function [14]; in addition, aberrant degradation of β-Dg through MMP-2 and MMP-9 has been recorded as a relevant

event observed in several tumor cell lines and in inflammatory diseases [16, 18].

In healthy blood cells, Dg has been described as forming part of actin-based structures such as filopodia and the lamellipodia of platelets [19] and neutrophils [20], contributing to the polarization of the activated forms of these cells. In the HL-60 leukemia cell line, in addition to a structural role, Dg exhibited an important role in modulating the differentiation process of neutrophils, increasing their expression level [21], while in Kasumi-1, another acute leukemia cell line, Dg is dispensable for macrophage differentiation, but is essential for their activities such as phagocytosis and migration, both actin-based functions [22].

The aim of the present study was to characterize the expression and subcellular distribution of Dgs of primary blast cells from patients with Acute Myeloid Leukemia (AML), as well as HL-60 and Kasumi-1 cell lines in relation to stem-progenitor cells from Healthy Individuals (HI). Additionally, we investigated the glycosylation status of α-Dg, as well as the expression levels of six of the known α-Dg modifying proteins in leukemia cells. Our results strongly suggest that the decreased expression and degradation, of Dg as well as the reduced glycosylation of α-Dg, are in accordance with the immaturity of the cells and contribute to leukemia pathogenesis. In support of this, the restoration of Dg expression in leukemia cell lines led to the reversion of some of the characteristics associated with the disease.

2. Materials and Methods

2.1. HL-60 and Kasumi-1 cell culture and differentiation

HL-60 (ATCC® CCL-240™) were cultured in Iscove's Modified Dulbecco's Medium (IMDM) and Kasumi-1 cells (ATCC® CRL-2724™) were cultured in RPMI-1640 medium supplemented with 10% Fetal Bovine Serum (FBS), 400 mM L-glutamine, 50 µM Gentamicin, 25 mM HEPES, 2 g/L sodium bicarbonate, 1 mM sodium pyruvate in a humid atmosphere of 5% CO_2 at 37°C. For differentiation into a neutrophil phenotype, HL-60 cells (HL-60 D) were differentiated with 1.3% (v/v) (DMSO) for 7 days [23], while for differentiation into macrophage-like cells, Kasumi-1 cells (Kasumi-1 D) were differentiated with 10^{-7} M 12-0-TetradecanoylPhorbol-13-Acetate (TPA) for 7 days [24]. In both cases, cell viability was assessed by exclusion of 0.2% Trypan Blue and was routinely >90% before and after differentiation.

2.2. Acute Myeloid Leukemia (AML) cells

Peripheral blood samples were obtained from 43 patients diagnosed with AML. Acute leukemia cells have classified in six main types (MI, M2, M3, M4, M5, and M6) defined according to (a) the direction of differentiation along one or more cell lines, and (b) the degree of maturation of the cells. Thus, M1, M2, and M3 exhibit predominantly granulocytic differentiation and differ from each another in terms of the extent and nature of granulocytic maturation [25].

They represent a group of patients with high peripheral blood blast counts who were treated either at the Hematology Unit at the Hospital General de México or Hospital Juárez de México. In each case, diagnosis was based on morphologic, immunophenotypic, and molecular analysis. All samples were obtained with signed informed consent by using a protocol approved by the Escuela Nacional de Medicina y Homeopatía, IPN, México. Patient characteristics are summarized in Table 1.

CD34+ cells were isolated from mononuclear cells from peripheral blood samples

using the Dynabeads CD34^{+} isolation kit cat. 11301D, according to the manufacturer's instructions (Invitrogen, Life Technologies, Carlsbad, CA, USA). Samples from harvested mobilized stem cells were used as stem-progenitor controls and they were donated from Banco Central de Sangre del Centro Médico Nacional "La Raza" after signing written informed consent.

2.3. Mobilization regimen and time of harvest

Thirty-three healthy allogenic stem cell donors underwent mobilization with hematopoietic Granulocyte Colony-Stimulating Factor (G-CSF; Neupogen, Amgen, München, Germany) with 10 μg/kg divided into two doses, administered subcutaneously (s.c.). Cells were harvested on the 5th day of mobilization. The remainder of the samples used for stem cell quantification was donated for this study.

2.4. CD34 positive cell count determination

CD34 positive cell counts were determined preprocedurally in the autologous donor's peripheral blood and in the leukapheresis product by flow cytometry (FACS Calibur; Becton Dickinson, Heidelberg, Germany). In 48 cases, counting was also done in peripheral blood 1 h after the leukapheresis procedure. The flow cytometric analysis followed the accepted protocol provided by the International Society of Haematology and Graft Engineering. Total Leukocyte Count (TLC) was performed in a calibrated automated cell counter (Sysmex XE 2100; Sysmex Corporation, Japan) using monoclonal CD34 antibody (clone 8G12; BD Biosciences, San Jose,, CA, USA) and CD45 (clone 2D1; BD Biosciences).

2.5. Immunofluorescence staining

Cells from leukemia samples as well as from cell lines (HL-60 and Kasumi-1) were adhered to poly-D-lysine-coated coverslips and after 60 min permeabilized and fixed with a mixture of 2% p-formaldehyde, 0.04% NP40 in the cytoskeleton-stabilizing solution PHEM and triton 0.2%. Captured optical sections [z] were quantified using ImageJ (NIH, Bethesda, MD, USA) [21]. Filopodia size and

number were detected using FiloDetect software from images taken by fluorescence microscopy as described previously [26]

2.6 Western blot analysis

Leukemia sample cells and cell lines were resuspended and lysed with a 2X lysis buffer (0.5% NP-40, 2 mM Na_3VO_4, PMSF) containing a protease inhibitor cocktail. Homogenates were sonicated 3 times for 15 sec. The protein concentrations were determined by the BCA method. The protein extract was mixed by loading buffer (Tris–HCl sodium dodecyl sulfate, β-mercaptoethanol, glycerol, bromophenol blue) and boiled for 5 minutes. Whole cell lysates were separated as described in [21].

2.7. Plasmids and transfection

Full-length mouse dystroglycan complementary DNA (cDNA) encoding α- and β-dystroglycans was subcloned into the pcDNA3 vector (Invitrogen Life Technologies, Carlsbad, CA, USA) with construct fidelity verified by nucleotide sequencing as described previously [27].

HL-60 or Kasumi-1 cells (2×10^6/mL) were transfected with 2 µg DNA mixed with 2 µg of pEGFP-N3 to mark the transfected cell population (Clontech, Mountain View, CA, USA) using a Nucleofector™ II electroporator (Amaxa), according to the manufacturer's recommendation (Lonza Walkersville, Inc., Walkersville, MD, USA). Cells were cultured in the presence of Neomycin at 800 µg/mL to select cells that expressed dystroglycans and at 400 µg/mL and to obtain stable cultures.

2.8. Quantitative Real-Time PCR

Total RNA was extracted from Kasumi-1 cells using Trizol Reagent (Life Technologies, Waltham, MA, USA) according to the manufacturer's instructions. One hundred ng of total RNA was subjected to Real-Time PCR performed in triplicate using KAPA SYBR FAST One-Step qRT-PCR kit; Kapa Biosystems, Wilmington, MA, USA) in a final volume of 20 µL. Quantitative assessment of mRNA expression was performed by Real-Time-RT-PCR (qRT-PCR) as described

in Supplemental Materials and Methods; a primer sequence table is also included in Supplemental Materials and Methods. Triplicate Ct values for Dg, POMGnT-2, POMT-1, POMT-2, LARGE, Fukutin, FKRP and GlycerAldehyde-3-Phosphate DeHydrogenase (GAPDH) were obtained from six different patients with the three different leukemia phenotypes.

2.9. Analysis of cell-surface antigens by immunofluorescence flow cytometry

Cells at 1 × 10^5/mL (100 µL) were incubated with monoclonal antibody for 30 min at 4ºC, washed twice with Phosphate-Buffered Saline (PBS) solution, and suspended for 30 min at 4°C in 100 µL of Alexa 488-conjugated goat anti-rabbit IgG (Molecular Probes Kallestad Laboratories, Inc., Austin, TX, USA) as previously described [21]. Results were presented as percentages of positive cells for each antigen.

2.10. Phagocytosis assays

Differentiated Kasumi-1 cells were allowed to interact at 37°C with Phalloidin-TRITC-labelled *Candida glabrata*, as described in [21].

2.11. MTT assay

Cell proliferation after transfection with the empty vector and Dg+ were measured by the (MTT) assay (ATCC® 30-1010K). HL-60 and Kasumi-1 cells (1 × 10^3/100 µL) were seeded in 96-well microplates and cultured for 9 days. A viability assay using Trypan Blue was assessed each day to ensure that survival was not compromised (minimal viability corresponded to 92% at day 9 for HL-60 cells and 80% for Kasumi-1 cells). After the incubation time, 20 µL of the MTT solution (5 mg/mL) was added to each well and incubated for another 3 h at 37°C. The formazan crystal formed by the living cells was dissolved with 150 µL of DMSO overnight. Then, Optical Density (OD) was measured using the Epoch Microplate Spectrophotometer (BioTek, Winooski, VT, USA) at 570 nm. The data were processed in GraphPad Prism 5 (GraphPad Software, La Jolla, CA, USA).

2.12. Statistical analysis

Statistical analysis was carried out with GraphPad Prism for Windows ver.5 software (GraphPad Software) Inc.). Relative protein expression and relative mRNA expression were analyzed with an unpaired Student *t* test. Statistical significance was defined as $p < 0.05$.

3. Results

3.1. Dystroglycan Distribution in Leukemia Primary Blasts and Cell Lines

To evaluate the subcellular distribution of Dg subunits, double immunofluorescence staining and confocal microscopy analysis on blasts of patients with AML (subtypes M1, M2, and M3; Table 2S), leukemia cell lines (HL-60 and Kasumi-1) compared to stem-progenitor cells from Healthy Individuals (HI) from mobilized cells were performed utilizing antibodies raised against α-Dg, β-Dg, and βDgpY892 revealed with Alexa-Fluor-488 secondary antibody. We analyzed images from five different patients corresponding to each subtype (M1, M2, and M3). However, as the subcellular distribution did not vary importantly, representative images of M1 subtype are described and included in Figure 1, while representative images from subtypes M2 and M3 appeared in Supplemental Figure 1S. Actin filaments were identified with Tetramethyl Rhodamine Iso-ThioCyanate (TRITC)-phalloidin. In the cells of HI (Figure 1 A), the α-Dg subunit displayed a punctate pattern distributed at the plasma membrane and scarce distribution in the cytoplasm where it co-localized with actin filaments and in the nucleus. This distribution was very similar to that observed in AML cells irrespective of the type of leukemia (M1, Figure 1B; M2 and M3, Supplemental Figure 1S). β-Dg and its phosphorylated form were observed with a homogeneous pattern in the all of the cells, including the nuclei of $CD34^{+}$ cells from individuals with leukemia.

The α-Dg distribution in HL-60 and Kasumi-1 cells was very similar to that described for cells from patients, while β-Dg distribution and its phosphorylated form were observed in the cytoplasm, plasma membrane, and nuclei (Figures 1C). In the cells of HI, β-DgpY892 was observed exhibiting a patchy pattern restricted to the plasma membrane and cytoplasm; this feature is the most relevant and consistent finding among the processed samples. Therefore, the important difference observed for dystroglycan distribution is related to the differing nuclear localization of β-DgpY892 in all leukemia cells compared to healthy CD34+ cells.

3.2. Dg Is Downregulated in Leukemia Cells

To characterize the expression pattern of α-Dg in primary leukemia blasts, we processed representative samples (n = 6) in triplicate of each of the three different phenotypes classified according to FAB (French-American-British group) as M1, M2, and M3 (Table 2S). These samples were analyzed using WB analysis with mouse monoclonal antibodies against α-Dg core protein (6C1), β-Dg (Mandag), and the β-Dg phosphorylated form (β-DgpY892). The α-Dg core protein revealed by the presence of a 70-kDa band observed in both the control group of HI as well as for AML cells. The use of β-Dg antibody (Mandag) confirmed comparable levels of β-Dg proteins among the leukemia samples but lower in relation to controls. A similar result was observed when the phosphorylated species of β-Dg was analyzed. The relative abundance of the protein was normalized with GAPDH as a loading control, demonstrating a statistical significant reduction (p <0.05) with all of the Dg species assayed in AML cells as compared to control (Figure 2A). We also assessed the Dg pattern expression in leukemia cell lines (HL-60 and Kasumi-1) by carrying out WB analysis; a 70-kDa band was detected with 6C1 antibody. A low-intensity band of 43 kDa using Mandag antibody was observed in leukemia cell line samples compared to HI. This same pattern was observed with a 43-kDa band when β-DgpY892 was evaluated (Figure 2B).

To corroborate the diminished level expression of dystroglycan in AML cells and leukemia cell lines observed by WB assays, we analyzed mRNA expression from M1, M2, and M3 leukemia primary blasts (n = 6 for each subtype) and leukemia cell lines by quantitative Reverse Transcription-PCR (qRT-PCR) (Figures 2C and 2D, respectively). mRNA expression of dystroglycans was significantly lower for AML primary blasts as well as for leukemia cells, respectively, compared to $CD34^+$ cells from HI (p <0.05), and this reduction appears to correlate with the immaturity of the cells.

In order to assess the effect of AML1-ETO on Sp1 transcription factor on *DAG* gene promotor regulation [28, 29], we processed, in triplicate, nuclear extracts from

leukemia cell lines and HeLa cells for WB assays using Sp1 antibody. The results revealed that Sp1 is reduced in leukemia cell lines compared to epithelial cervix carcinoma cells (HeLa) (Figure 2E).

3.3. Changes in Dystroglycan Post-translational Modification

To characterize the biochemical properties of glycosylated α-Dg species in primary leukemia blasts, we processed representative samples of three different phenotypes classified according to FAB as M1, M2 and M3 by WB analysis with mouse monoclonal antibodies IIH6C4 mouse monoclonal antibodies. This antibody recognizes glycosylated epitopes on α-Dg, as well as revealing hypoglycosylation in the absence of epitopes for the antibody when compared to the total α-Dg core protein levels [30].

WB with IIH6C4 detected 140-kDa bands in the control group (HI), the reactivity of this antibody for the 140 kDa and the lower bands were reduced in leukemia patients' cells relative to controls (arrow). The relative abundance of the protein was normalized with GAPDH as loading control showing a statistical significance reduction (p <0.05) with all the Dg species assayed in AML cells as compared to control (Figure 3A). We also assessed the glycosylation state of α-Dg within the two leukemia cell lines (HL-60 and Kasumi-1) by carrying out WB analysis, which was revealed with a band of 140 kDa observed using IIH6C4. A statistically significant reduction in intensity of the 140-kDa band (p <0.05) was observed in samples from the two leukemia cell lines (Figure 3B). Other bands of α-Dg protein with lower molecular weight can be visualized with long exposure times.

According to our WB results in cell lines and leukemia cells from patients, we inferred that there might be Dg glycosylation defects in α-subunit, as has been observed in cancer cell lines from solid tissue [31]. Thus, we assessed the expression level of mRNA of some of the main enzymes that modulate Dg glycosylation, including POMGnT1, POMT1, POMT2, LARGE, FKTN, and FKRP, [11, 32] by carrying out qRT-PCR analysis of these six enzymes. Figure 3C shows

a heterogeneous pattern expression of the six glycosyltransferases for AML leukemia cells; POMGNT-1, POMT-1, POMT-2, and Fukutin are expressed to a greater degree in leukemia samples than in HI, except for LARGE and FKRP. While the qRT-PCR assays of the six glycosyltransferases (POMGnT1, POMT1, POMT2, LARGE, FKTN, and FKRP) in AML cell lines (Figure 3D) demonstrates the relative reduction in the expression of the six glycosyltransferases in both HL-60 and Kasumi-1 cell lines. In HL-60 cells, nearly all the enzymes assayed are expressed with lower values than those observed for Kasumi-1 cells- LARGE mRNA levels are similar for both cell lines, while Fukutin is nearly absent for Kasumi-1 cells.

3.4. Restoration of Dg Levels in Leukemia Cell Lines

To investigate whether restoration of Dg was sufficient to reduce proliferation and to improve differentiation and the functional properties of leukemia cells, we modified HL-60 and Kasumi-1 cells to stably express Dg (Dg+). HL-60 cells showed good expression of the transgene at the protein level, but to a lesser extent in Kasumi-1 cells observed by a 70-kDa band corresponding to β-Dg and GFP; however, qRT-PCR results were consistent for both cell lines (Supplemental Figure 1).

The proliferation process was directly evaluated by MTT assays from HL-60 and Kasumi-1 synchronized cultures; our results revealed that cells expressing (Dg+) diminished their proliferation compared to cells that were transfected with the Empty Vector (EV), suggesting that Dg modulates the proliferation process for both cell lines (Figure 4A). The differentiation process triggered by DMSO typical and functional characteristics will be present, such as phagocytic capability. Therefore, after 7 days of treatment with DMSO, the differentiated cells might phagocyte *C. glabrata,* in contrast to non-differentiated cells; however, to our surprise, HL-60 non-differentiated cells that were overexpressing Dg (Dg+ ND) acquired the phagocytic capability at the same level as control differentiated cells (HL-60 D)

(Figure 4B). This characteristic reached nearly 70% of the differentiated population overexpressing Dg (Dg+ D). On the other hand, Kasumi-1 cells did not show a significant difference between the phagocytic characteristic between differentiated (Dg+ D) and non-differentiated (Dg+ ND) cells that were overexpressing Dg; a difference was found between the differentiated cells overexpressing Dg (Dg+ D) and the Empty Vector (EV D) (Figure 4C).

Finally, to corroborate whether the phagocytic characteristic was in accordance with the differentiation process, we evaluated by flow cytometer the presence of CD11b, which is a typical differentiation marker for neutrophil lineage. Our results revealed that CD11b expression was present in cells stably transfected with EV, Dg+, or non-transfected cells treated with DMSO and again untreated Dg overexpressing cells (Figure 4E). Kasumi-1 cells treated with PMA were differentiated to macrophage lineage, which was corroborated by the detection of CD68 at the surface of the cells. This marker was present at the surface of differentiated cells whether or not they overexpressed Dg (Figure 4F).

3.5. Dystroglycan Promotes Filopodial Formation in Leukemia Cell Lines

Previously, we reported that dystroglycan small interfering RNA (siRNA) decreased filopodia number and length in HL-60 and Kasumi-1 cells, as well as the functions related with actin-based structures [21, 22]. Therefore, F-actin from HL-60 and Kasumi-1 cells overexpressing Dg and controls were labelled with phalloidin to evaluate relative fluorescence units and number and length of filopodia during the differentiation process.

Panel A depicts the morphology of HL-60 cells through the differentiation process triggered by DMSO; filopodia were more evident on days 5 and 8 of treatment in Dg+ HL-60 cells. Panel B illustrates the morphology displayed by Dg+ and EV of Kasumi-1 cells during PMA treatment. The insets present filopodia detected by the software (observed in green); the number and length of these structures, as well as

F-actin intensity, were quantified along the differentiation process for both cell types.

Along the differentiation process (7 days), HL-60 cells did not exhibit an important difference related with F-actin content or filopodia length, however, we observed an increase in the number of filopodia in Dg+ cells, which is more evident at the end of the differentiation process (Figure 5A).

For Kasumi-1 cells, relative F-actin content is apparently heterogeneous and does not increase as the cell differentiates. The length of filopodia showed a short increase as the cell is differentiated; however, there is no difference between Dg+ cells and the controls (EV). On the other hand, the number of filopodia is increased in accordance with the advance of the differentiation process, and the values are statistically significant for days 5 and 8 of differentiation (Figure 5B).

4. Discussion

In the present study, we show, to our knowledge for the first time, the expression pattern and subcellular distribution of Dg in primary blasts from patients with acute leukemia. In this pathology, protein levels corresponding to the Dg core protein, the glycosylated species of α-Dg, as well as for β-Dg and its phosphorylated form demonstrated reduced expression. This diminution does not correlate universally with clinical severity, as reported for other systems [33], in contrast to the transcriptional level detected with qRT-PCR assays.

The AML1-ETO fusion protein indicates Acute Myeloid Leukemia (AML) with t(8;21)(q22;q22), present in10–15% of all AML cases [34], although AML is induced unless secondary mutations take place [35]. Specificity protein 1 transcription factor (Sp1) regulates the *Dag1* gene [29] and interacts with AML1-ETO, leading to Sp1 transactivity inhibition [28]. We confirmed the diminished expression of Sp1 in leukemia cell lines by WB assay and this might explain low level of Dg mRNA low levels.

The presence of Dg in the nucleus has been recently described, forming part of the nucleoskeleton, as well as modulating the transcriptionally active regions [36]. The presence of β-DgpY892 in the nucleus of leukemia cells might be indicative of active ubiquitination, which in turn might exacerbate dysregulation in proliferation and differentiation processes, as has been proposed for prostate [37].

Because we did not use a Furin inhibitor in the present study, a diminished relative molecular weight of α-Dg (140 kDa) was evident compared to the data reported in our previous studies for HL-60 and Kasumi-1 cells (160 kDa) [21, 22]. Thus, we hypothesize that proteolysis of the β-Dg ectodomain [38] or of α-Dg's N-terminal portion [39-41] produced by Matrix MetalloProteinases (MMP) Furin and γ-secretase [42], respectively, may contribute to the pathophysiology of the AML, as these have been implicated in cancer progression in other systems [43, 44]. Recently, it was established that hypoglycosylation severely alters α-Dg's capability to bind to ECM partners, facilitating its degradation by MMP-2 or by other enzymes not identified to date [45]; additionally, in some patients affected by

dystroglycanopathy, an important reduction of the Dg core protein was identified [46]. These events are in accordance with our results, in that we simultaneously observed a significant reduction in glycosylated α-Dg forms, as well as a reduction of Dg core protein. On the other hand, the cleavage of β-Dg due to MetalloProteinases (MP) generates a 31-kDa fragment that is directed to the proteasome for degradation [39]; however, this form was not evident for the samples processed in the present study.

A smaller α-Dg form was also observed (110 kDa) regardless of the source of the sample (patient or cell line); this form should not be detected by the carbohydrate-dependent IIH6 antibody, suggesting alteration in α-Dg glycosylation and loss of receptor function, as has been described for skeletal muscle in patients with dystroglycanopathy [30]. In support of these findings, we performed the quantification of six of the enzymes responsible for O-linked carbohydrate modifications of the α-Dg mucin domain that, in turn, modulate laminin anchoring, because similar defects have been observed in cancer cell lines [13, 14, 31, 39]. Results derived from AML blast cells as well as from leukemia cell lines converged in diminished LARGE expression. In some cancers, methylation changes at the promoter of this glycosylation enzyme leads to the loss of its protein expression [15]. The presence of non functionally-glycosylated α-Dg might contribute to the activity of MEK and AKT, and is responsible for poor clinical outcomes, as previously suggested [13].

Dg glycosylation regulated via N- or O- glycosylation sites [32] is a requirement for cells to bind to a wide range of ECM components to control cell survival, proliferation, and differentiation via cell surface receptors [47]. We have demonstrated that Dg glycosylation is highly regulated during the differentiation process of blood tissue cells, affecting their implicit functions [21, 22]. In the present study, we show that Dg glycosylation is differentially regulated and a failure in the glycosylation of laminin exists as a biochemical characteristic of acute leukemia cells, although we did not explore LARGE overexpression, which might partially rescue functions related to α-Dg glycosylation.

AML is a molecular and clinical heterogeneous disease [48] and, although there is

a direct correlation between AML cases with mutations (8:21) and the quantity of Dgs, the most important factor in the presentation of the disease might be attributed to the numerous defects found in terms of the quality of the Dgs system. Therefore, restoration of dystroglycans by stably transfecting leukemia cell lines (HL-60 and Kasumi-1 cells), with a plasmid expressing Dg nearly recovering the healthy phenotype as the proliferation process was reduced; the differentiation process, as well as actin-based functions (phagocytosis), were increased, demonstrating the importance of Dg structural and signalling roles in acute leukemia pathophysiology.

5. Conclusion

Our results strongly suggest that the balance and integrity between the dystroglycan alpha and beta subunits are indispensable and responsible for the cell differentiation and proliferation in acute leukemia cells. Further studies will be needed to determine whether the Dg could be useful as a potential biomarker not only to diagnose leukemia, but also to determine the prognosis of the disease.

Authors' contribution

DC designed the study and analyzed the data. LA-R, TB-G, and IM-V performed the experiments. DC, AM-T, BC, SW analyzed and discussed the results. DC and SW wrote the manuscript.

Conflict of interest

The authors declare no competing financial interests.

Acknowledgments

We thank Dr. Miguel Cruz-Rico and Dr. Mónica Tejeda-Romero from Hospital Juárez for patients' samples facilities.

This work was supported by CONACYT-México grant no.167178.

References

1. Ibraghimov-Beskrovnaya, O., J.M. Ervasti, C.J. Leveille, C.A. Slaughter, S.W. Sernett, and K.P. Campbell. Primary structure of dystrophin-associated glycoproteins linking dystrophin to the extracellular matrix. Nature, 1992. **355**(6362): p. 696-702.

2. Ervasti, J.M. and K.P. Campbell. A role for the dystrophin-glycoprotein complex as a transmembrane linker between laminin and actin. J Cell Biol, 1993. **122**(4): p. 809-823.

3. Martin, P.T. Dystroglycan glycosylation and its role in matrix binding in skeletal muscle. Glycobiology, 2003. **13**(8): p. 55R-66R.

4. Winder, S.J. The membrane-cytoskeleton interface: the role of dystrophin and utrophin. J Muscle Res Cell Motil, 1997. **18**(6): p. 617-629.

5. Kanagawa, M., D.E. Michele, J.S. Satz, R. Barresi, H. Kusano, T. Sasaki, R. Timpl, M.D. Henry, and K.P. Campbell. Disruption of perlecan binding and matrix assembly by post-translational or genetic disruption of dystroglycan function. FEBS Lett, 2005. **579**(21): p. 4792-4796.

6. Streuli, C.H., C. Schmidhauser, N. Bailey, P. Yurchenco, A.P. Skubitz, C. Roskelley, and M.J. Bissell. Laminin mediates tissue-specific gene expression in mammary epithelia. J Cell Biol, 1995. **129**(3): p. 591-603.

7. Patarroyo, M., K. Tryggvason, and I. Virtanen. Laminin isoforms in tumor invasion, angiogenesis and metastasis. Semin Cancer Biol, 2002. **12**(3): p. 197-207.

8. Moore, C.J. and S.J. Winder. The inside and out of dystroglycan post-translational modification. Neuromuscul Disord, 2012. **22**(11): p. 959-965.
9. Spence, H.J., A.S. Dhillon, M. James, and S.J. Winder. Dystroglycan, a scaffold for the ERK-MAP kinase cascade. EMBO Rep, 2004. **5**(5): p. 484-489.
10. Taniguchi-Ikeda, M., I. Morioka, K. Iijima, and T. Toda. Mechanistic aspects of the formation of alpha-dystroglycan and therapeutic research for the treatment of alpha-dystroglycanopathy: a review. Mol Aspects Med, 2016. **51**: p. 115-124.
11. Hewitt, J.E. Abnormal glycosylation of dystroglycan in human genetic disease. Biochim Biophys Acta, 2009. **1792**(9): p. 853-861.
12. Longman, C., M. Brockington, S. Torelli, C. Jiménez-Mallebrera, C. Kennedy, N. Khalil, L. Feng, R.K. Saran, T. Voit, L. Merlini, C.A. Sewry, S.C. Brown, and F. Muntoni. Mutations in the human LARGE gene cause MDC1D, a novel form of congenital muscular dystrophy with severe mental retardation and abnormal glycosylation of alpha-dystroglycan. Hum Mol Genet, 2003. **12**(21): p. 2853-2861.
13. Bao, X., M. Kobayashi, S. Hatakeyama, K. Angata, D. Gullberg, J. Nakayama, M.N. Fukuda, and M. Fukuda. Tumor suppressor function of laminin-binding alpha-dystroglycan requires a distinct beta3-N-acetylglucosaminyltransferase. Proc Natl Acad Sci U S A, 2009. **106**(29): p. 12109-12114.
14. de Bernabe, D.B., K. Inamori, T. Yoshida-Moriguchi, C.J. Weydert, H.A. Harper, T. Willer, M.D. Henry, and K.P. Campbell. Loss of alpha-dystroglycan laminin binding in epithelium-derived cancers is caused by silencing of LARGE. J Biol Chem, 2009. **284**(17): p. 11279-11284.
15. Akhavan, A., O.L. Griffith, L. Soroceanu, D. Leonoudakis, M.G. Luciani-Torres, A. Daemen, J.W. Gray, and J.L. Muschler. Loss of cell-surface laminin anchoring promotes tumor growth and is associated with poor clinical outcomes. Cancer Res, 2012. **72**(10): p. 2578-2588.

16. Sgambato, A. and A. Brancaccio. The dystroglycan complex: from biology to cancer. J Cell Physiol, 2005. **205**(2): p. 163-169.
17. Muschler, J., D. Levy, R. Boudreau, M. Henry, K. Campbell, and M.J. Bissell. A role for dystroglycan in epithelial polarization: loss of function in breast tumor cells. Cancer Res, 2002. **62**(23): p. 7102-7109.
18. Court, F.A., D. Zambroni, E. Pavoni, C. Colombelli, C. Baragli, G. Figlia, L. Sorokin, W. Ching, J.L. Salzer, L. Wrabetz, and M.L. Feltri. MMP2-9 cleavage of dystroglycan alters the size and molecular composition of Schwann cell domains. J Neurosci, 2011. **31**(34): p. 12208-12217.
19. Cerecedo, D., D. Martínez-Rojas, O. Chávez, F. Martínez-Pérez, F. García-Sierra, A. Rendón, D. Mornet, and R. Mondragón. Platelet adhesion: structural and functional diversity of short dystrophin and utrophins in the formation of dystrophin-associated-protein complexes related to actin dynamics. Thromb Haemost, 2005. **94**(6): p. 1203-1212.
20. Cerecedo, D., B. Cisneros, P. Gómez, and I.J. Galván. Distribution of dystrophin- and utrophin-associated protein complexes during activation of human neutrophils. Exp Hematol, 2010. **38**(8): p. 618-628, e613.
21. Martínez-Zárate, A.D., I. Martínez-Vieyra, L. Alonso-Rangel, B. Cisneros, S.J. Winder, and D. Cerecedo. Dystroglycan depletion inhibits the functions of differentiated HL-60 cells. Biochem Biophys Res Commun, 2014. **448**(3): p. 274-280.
22. Escárcega-Tame, M.A., I. Martínez-Vieyra, L. Alonso-Rangel, B. Cisneros, S.J. Winder, and D. Cerecedo. Dystroglycan depletion impairs actin-dependent functions of differentiated Kasumi-1 cells. PLOS ONE, 2015. **10**(12): p. e0144078.
23. Collins, S.J., F.W. Ruscetti, R.E. Gallagher, and R.C. Gallo. Terminal differentiation of human promyelocytic leukemia cells induced by dimethyl sulfoxide and other polar compounds. Proc Natl Acad Sci U S A, 1978. **75**(5): p. 2458-2462.

24. Koeffler, H.P., M. Bar-Eli, and M. Territo. Phorbol diester-induced macrophage differentiation of leukemic blasts from patients with human myelogenous leukemia. J Clin Invest, 1980. **66**(5): p. 1101-1108.

25. Bennett, J.M., D. Catovsky, M.T. Daniel, G. Flandrin, D.A. Galton, H.R. Gralnick, and C. Sultan. Proposals for the classification of the acute leukaemias. French-American-British (FAB) co-operative group. Br J Haematol, 1976. **33**(4): p. 451-458.

26. Nilufar, S., A.A. Morrow, J.M. Lee, and T.J. Perkins. FiloDetect: automatic detection of filopodia from fluorescence microscopy images. BMC Syst Biol, 2013. **7**: p. 66.

27. Batchelor, C.L., J.R. Higginson, Y.J. Chen, C. Vanni, A. Eva, and S.J. Winder. Recruitment of Dbl by ezrin and dystroglycan drives membrane proximal Cdc42 activation and filopodia formation. Cell Cycle, 2007. **6**(3): p. 353-363.

28. Wei, H., X. Liu, X. Xiong, Y. Wang, Q. Rao, M. Wang, and J. Wang. AML1-ETO interacts with Sp1 and antagonizes Sp1 transactivity through RUNT domain. FEBS Lett, 2008. **582**(15): p. 2167-2172.

29. Rettino, A., F. Rafanelli, G. Genovese, M. Goracci, R.A. Cifarelli, A. Cittadini, and A. Sgambato. Identification of Sp1 and GC-boxes as transcriptional regulators of mouse *Dag1* gene promoter. Am J Physiol Cell Physiol, 2009. **297**(5): p. C1113-C1123.

30. Michele, D.E., R. Barresi, M. Kanagawa, F. Saito, R.D. Cohn, J.S. Satz, J. Dollar, I. Nishino, R.I. Kelley, H. Somer, V. Straub, K.D. Mathews, S.A. Moore, and K.P. Campbell. Post-translational disruption of dystroglycan-ligand interactions in congenital muscular dystrophies. Nature, 2002. **418**(6896): p. 417-422.

31. Martin, L.T., M. Glass, E. Dosunmu, and P.T. Martin. Altered expression of natively glycosylated alpha dystroglycan in pediatric solid tumors. Hum Pathol, 2007. **38**(11): p. 1657-1668.

32. Barresi, R. and K.P. Campbell. Dystroglycan: from biosynthesis to pathogenesis of human disease. J Cell Sci, 2006. **119**(Pt 2): p. 199-207.

33. Jiménez-Mallebrera, C., S. Torelli, L. Feng, J. Kim, C. Godfrey, E. Clement, R. Mein, S. Abbs, S.C. Brown, K.P. Campbell, S. Kroger, B. Talim, H. Topaloglu, R. Quinlivan, H. Roper, A.M. Childs, M. Kinali, C.A. Sewry, and F. Muntoni. A comparative study of alpha-dystroglycan glycosylation in dystroglycanopathies suggests that the hypoglycosylation of alpha-dystroglycan does not consistently correlate with clinical severity. Brain Pathol, 2009. **19**(4): p. 596-611.

34. Peterson, L.F. and D.E. Zhang. The 8;21 translocation in leukemogenesis. Oncogene, 2004. **23**(24): p. 4255-4262.

35. Yuan, Y., L. Zhou, T. Miyamoto, H. Iwasaki, N. Harakawa, C.J. Hetherington, S.A. Burel, E. Lagasse, I.L. Weissman, K. Akashi, and D.E. Zhang. AML1-ETO expression is directly involved in the development of acute myeloid leukemia in the presence of additional mutations. Proc Natl Acad Sci U S A, 2001. **98**(18): p. 10398-10403.

36. Martínez-Vieyra, I.A., A. Vásquez-Limeta, R. González-Ramírez, S.L. Morales-Lázaro, M. Mondragón, R. Mondragón, A. Ortega, S.J. Winder, and B. Cisneros. A role for beta-dystroglycan in the organization and structure of the nucleus in myoblasts. Biochim Biophys Acta, 2013. **1833**(3): p. 698-711.

37. Mitchell, A., G. Mathew, T. Jiang, F.C. Hamdy, S.S. Cross, C. Eaton, and S.J. Winder. Dystroglycan function is a novel determinant of tumor growth and behavior in prostate cancer. Prostate, 2013. **73**(4): p. 398-408.

38. Losasso, C., F. Di Tommaso, A. Sgambato, R. Ardito, A. Cittadini, B. Giardina, T.C. Petrucci, and A. Brancaccio. Anomalous dystroglycan in carcinoma cell lines. FEBS Lett, 2000. **484**(3): p. 194-198.

39. Singh, J., Y. Itahana, S. Knight-Krajewski, M. Kanagawa, K.P. Campbell, M.J. Bissell, and J. Muschler. Proteolytic enzymes and altered glycosylation modulate dystroglycan function in carcinoma cells. Cancer Res, 2004. **64**(17): p. 6152-6159.

40. Saito, F., Y. Saito-Arai, A. Nakamura-Okuma, M. Ikeda, H. Hagiwara, T. Masaki, T. Shimizu, and K. Matsumura. Secretion of N-terminal domain of

alpha-dystroglycan in cerebrospinal fluid. Biochem Biophys Res Commun, 2011. **411**(2): p. 365-369.

41. Hesse, C., I. Johansson, N. Mattsson, D. Bremell, U. Andreasson, A. Halim, R. Anckarsater, K. Blennow, H. Anckarsater, H. Zetterberg, G. Larson, L. Hagberg, and A. Grahn. The N-terminal domain of alpha-dystroglycan, released as a 38 kDa protein, is increased in cerebrospinal fluid in patients with Lyme neuroborreliosis. Biochem Biophys Res Commun, 2011. **412**(3): p. 494-499.

42. Leocadio, D., A. Mitchell, and S.J. Winder. Gamma-secretase dependent nuclear targeting of dystroglycan. J Cell Biochem, 2016. **117**(9): p. 2149-2157.

43. Bassi, D.E., H. Mahloogi, R. López De Cicco, and A. Klein-Szanto. Increased furin activity enhances the malignant phenotype of human head and neck cancer cells. Am J Pathol, 2003. **162**(2): p. 439-447.

44. Egeblad, M. and Z. Werb. New functions for the matrix metalloproteinases in cancer progression. Nat Rev Cancer, 2002. **2**(3): p. 161-174.

45. Sbardella, D., R. Inzitari, F. Iavarone, M. Gioia, S. Marini, F. Sciandra, M. Castagnola, P.E. Van den Steen, G. Opdenakker, B. Giardina, A. Brancaccio, M. Coletta, and M. Bozzi. Enzymatic processing by MMP-2 and MMP-9 of wild-type and mutated mouse beta-dystroglycan. IUBMB Life, 2012. **64**(12): p. 988-994.

46. Humphrey, E.L., E. Lacey, L.T. Le, L. Feng, F. Sciandra, C.R. Morris, J.E. Hewitt, I. Holt, A. Brancaccio, R. Barresi, C.A. Sewry, S.C. Brown, and G.E. Morris. A new monoclonal antibody DAG-6F4 against human alpha-dystroglycan reveals reduced core protein in some, but not all, dystroglycanopathy patients. Neuromuscul Disord, 2015. **25**(1): p. 32-42.

47. Vachon, P.H. Integrin signaling, cell survival, and anoikis: distinctions, differences, and differentiation. J Signal Transduct, 2011. **2011**: p. 738137.

48. Dohner, H., D.J. Weisdorf, and C.D. Bloomfield. Acute myeloid leukemia. N Engl J Med, 2015. **373**(12): p. 1136-1152.

Figure Legends

Figure 1. Subcellular distribution of dystroglycans in acute leukemia cells.
CD34+ stem-progenitor cells from Healthy Individuals (HI) Panel A, primary blast cells from M1 in patients with Acute Myeloid Leukemia (AML-1) Panel B, and HL-60, and Kasumi-1 Panel C, were placed on glass coverslips were processed for double immunofluorescence microscopy using anti-dystroglycan antibodies (green), phalloidin (red) to visualize the F-actin network and DAPI (blue) for nuclei were analyzed by confocal microscopy. Bar = 10 μm.

Figure 2. Pattern of expression of dystroglycans in acute leukemia cells.
Panel A. Total lysates of primary blast cells from M1, M2, and M3 in patients with Acute Myeloid Leukemia (AML-1, AML-M2, AML-3) were analyzed by Western Blot (WB) utilizing antibodies against the α-Dg core protein (6C-1), β-Dg (Mandag), and βDgpY892. Quantitative analysis using GAPDH as loading control is shown. Values depicted are mean ± Standard Error of the Mean (SEM) from three independent experiments (n = 3), respectively. *P <0.005; **P <0.003. Panel B. Total lysates of CD34+ stem-progenitor cells from Healthy Individuals (HI), HL-60, and Kasumi-1 cells were analyzed as mentioned previously. Panel C. Messenger RNA (mRNA) expression of dystroglycan was examined by quantitative Reverse Transcription-PCR (qRT-PCR) in primary blast cells from M1, M2, and M3 in patients with Acute Myeloid Leukemia (AML-1, AML-M2, AML-3) compared to $CD34^+$ stem-progenitor cells from Healthy Individuals (HI). Values shown are mean ± Standard Error of the mean (SEM) from six different patients performed in triplicate, respectively. Panel D. Messenger RNA (mRNA) expression of dystroglycan was examined by quantitative Reverse Transcription-PCR (qRT-PCR) in primary blast cells from HL-60 and Kasumi-1 cells compared to $CD34^+$ stem-progenitor cells from Healthy Individuals (HI). Values depicted are mean ± Standard error of the Mean (SEM) from three independent experiments (n = 3), respectively. *P <0.05; **P <0.03. Panel E. Total extracts from HeLa, and Western

Blot (WB) utilizing an antibody against Sp1 and actin as a loading control analyzed nuclear extracts from HL-60 and Kasumi-1 cells.

Figure 3. Deregulation in α-Dg glycosylation in leukemia cells.
Panel A. Total lysates of primary blast cells from M1, M2, and M3 in patients with Acute Myeloid Leukemia (AML-1, AML-M2, AML-3) were analyzed by Western Blot (WB) utilizing an antibody against the central mucin-like region of α-Dg (IIH6C4). Quantitative analysis using GAPDH as loading control is shown. Panel B. Total lysates of CD34+ stem-progenitor cells from Healthy Individuals (HI), HL-60, and Kasumi-1 cells were analyzed as previously mentioned. Values shown are mean ± Standard Error of the Mean (SEM) from three independent experiments (n = 3), respectively. *P <0.005; **P <0.003. Panel C. Messenger RNA (mRNA) expression of dystroglycan was examined by quantitative Reverse Transcription-PCR (qRT-PCR) in primary blast cells from M1, M2, and M3 in patients with Acute Myeloid Leukemia (AML-M1, AML-M2, AML-M3) compared to $CD34^+$ stem-progenitor cells from Healthy Individuals (HI). Values depicted are mean ± Standard Error of the Mean (SEM) from six different patients performed in triplicate, respectively. Panel D. Messenger RNA (mRNA) expression of the main putative glycosyltransferases (POMGnT1, POMT1, POMT2 LARGE, FKRP, and Fukutin) in HL-60 and Kasumi-1 cells compared to $CD34^+$ stem-progenitor cells from HI was analyzed as described previously. Values shown are mean ± SEM from three independent experiments (n = 3), respectively. *P <0.05.

Figure 4. Dystroglycan re-expression contributed to correct leukemic phenotype. HL-60 cells, Panel A; and Kasumi-1 cells Panel B; transfected with Empty Vector (EV) and Dg overexpressing vector (Dg^+) were processed for MTT assay for 9 days at different intervals. Cells overexpressing Dg+ diminished their proliferation rates. HL-60 and Kasumi-1 cells transfected with EV and Dg overexpressing vector (Dg^+) were evaluated for their phagocytic ability by internalization of *Candida glabrata* labelled with phalloidin–TRITC Panel C and panel D respectively. This function was more evident for Dg+ cells without regarding the cell line compared to

controls. Error bars show ± Standard Error of the Mean (SEM) based on a total of three experiments. **P* <0.05; ***P* <0.03.

HL-60 cells, Panel E and Kasumi-1 cells, Panel F transfected with Empty Vector (EV) and Dg overexpressing vector (Dg^+) were processed by flow cytometer using antibodies against differentiation markers CD11b and CD68 for neutrophils and macrophages respectively. The differentiation process was present in Dg+ cells, even in non-treated cells. Error bars show ± SEM, based on a total of three experiments. **P* <0.05.

Figure 5. Dystroglycan overexpression promotes filopodia formation in acute leukemic cells. Panel A. HL-60, or Panel B. Kasumi-1 cells, transfected with Empty Vector (EV) and Dg overexpressing vector (Dg+) were analyzed by confocal microscopy to evaluate morphological changes in response to the increase of dystroglycan during the differentiation process (8 days). Bar = 10 μm.

Number and length of filopodia was quantified by FiloDetect software in HL-60 and Kasumi-1 cells transfected with Dg (Dg+). Values shown are mean ± Standard Error of the Mean (SEM) from three independent experiments each measuring 20 cells, compared to Empty Vector (EV) controls. ****P* <0.001.

Supplemental Figure 1

Subcellular distribution of dystroglycans in acute leukemia cells.

Panel A. Primary blast cells from M2, and M3 in patients with Acute Myeloid Leukemia (AML-M2, AML-3) placed on glass coverslips were processed for double immunofluorescence microscopy using anti-dystroglycan antibodies (green), phalloidin (red) to visualize the F-actin network and DAPI (blue) for nuclei were analyzed by confocal microscopy. Bar = 10 μm.

Supplemental Figure 2

HL-60 and Kasumi-1 cells were transfected with vectors expressing Dg (Dg+) or

with Empty Vector (EV). Total HL-60 and Kasumi-1 cell extracts were processed for Western Blot (WB) utilizing an antibody against β-dystroglycan; corresponding bands were observed at 42 kDa and 70 kDa. Densitometry analysis demonstrated β-Dg expressed in cells transfected with a Dg+ vector as compared with cells transfected with a control EV. Values shown are mean ± Standard Error of the Mean (SEM) from three independent experiments (n = 3), respectively. $^{*}P$ <0.05; $^{**}P$ <0.03.

Figure 1
Click here to download high resolution image

- Figure 1-

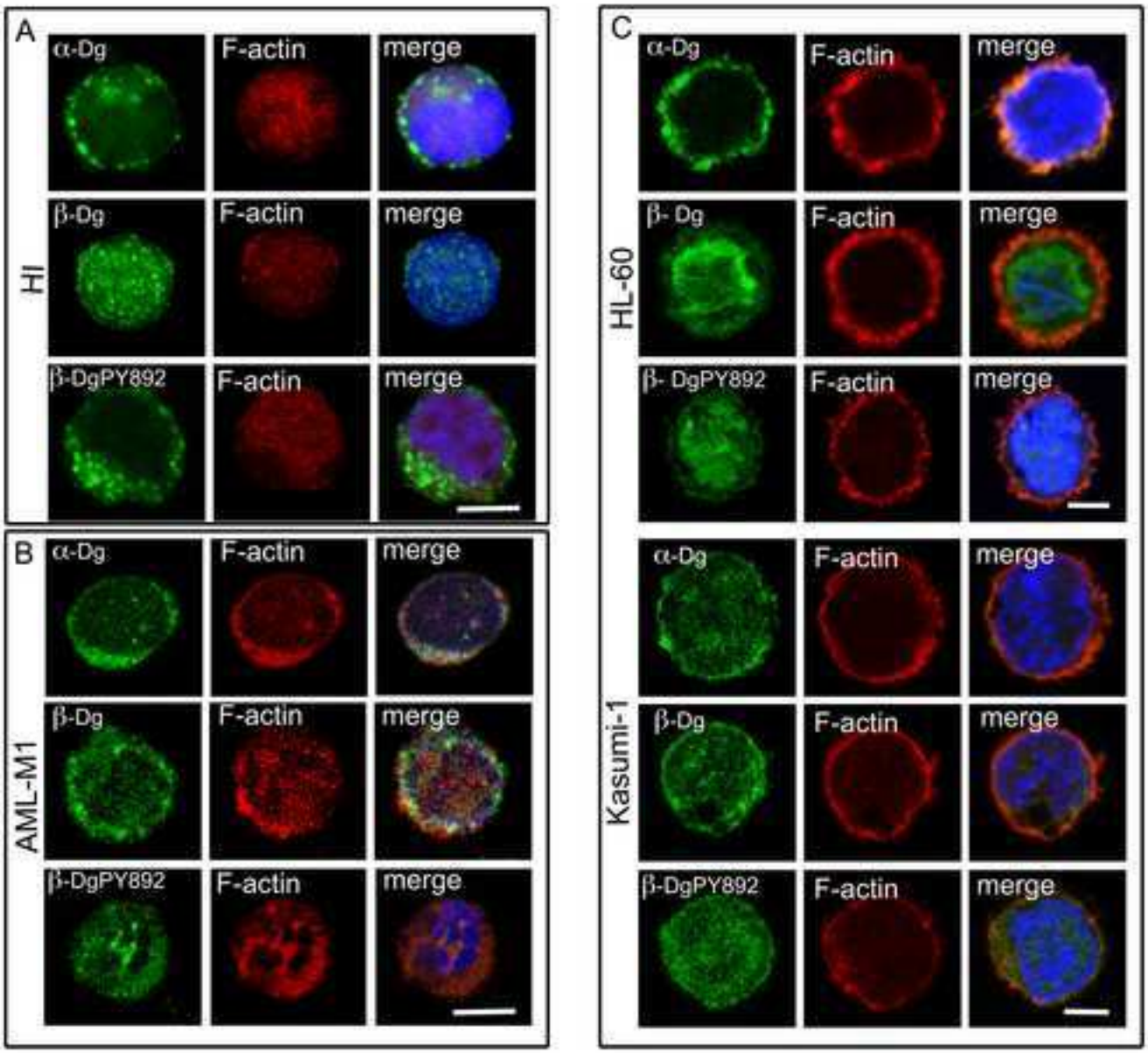

Figure 2

Click here to download high resolution image

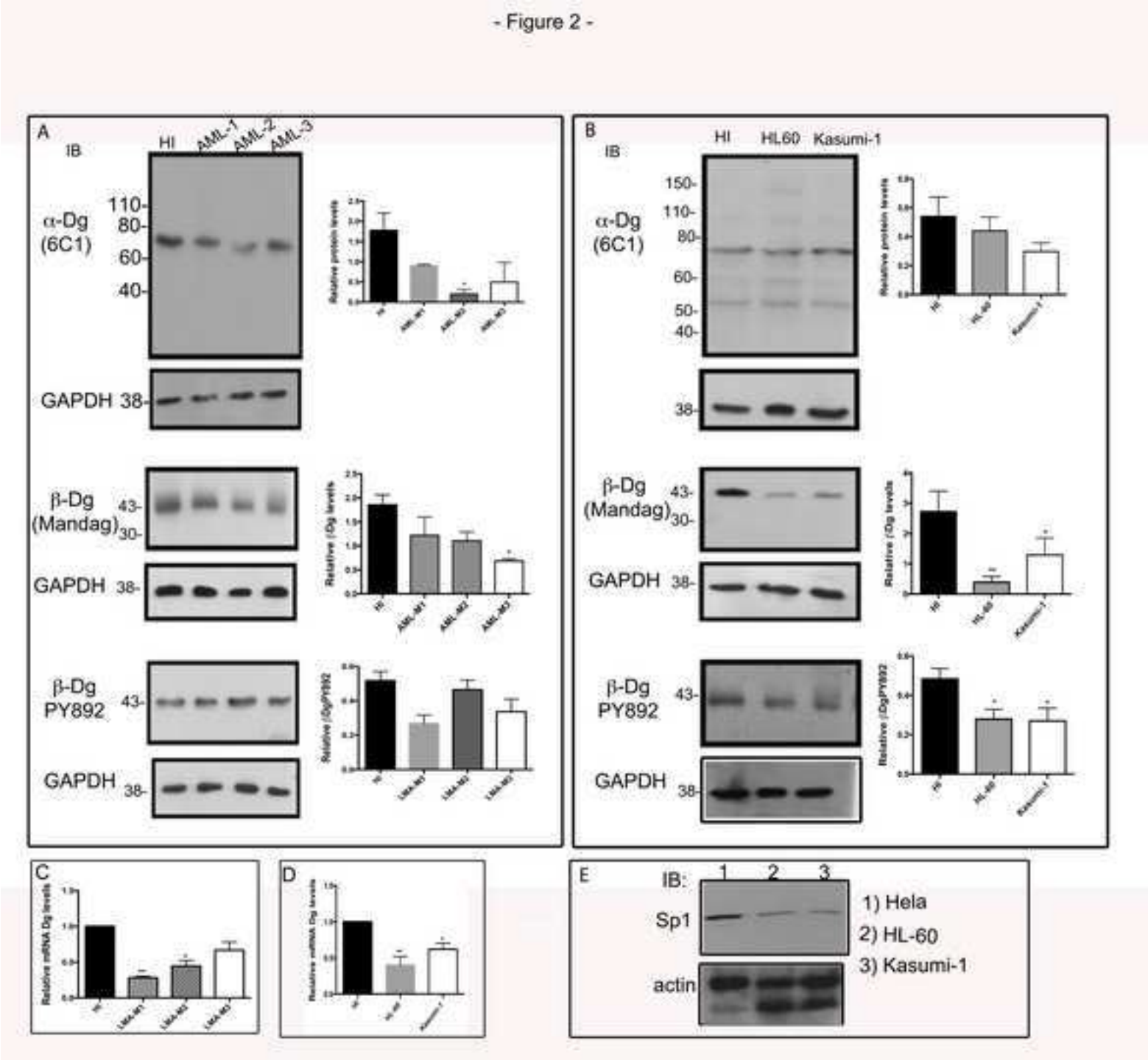

Figure 3

Click here to download high resolution image

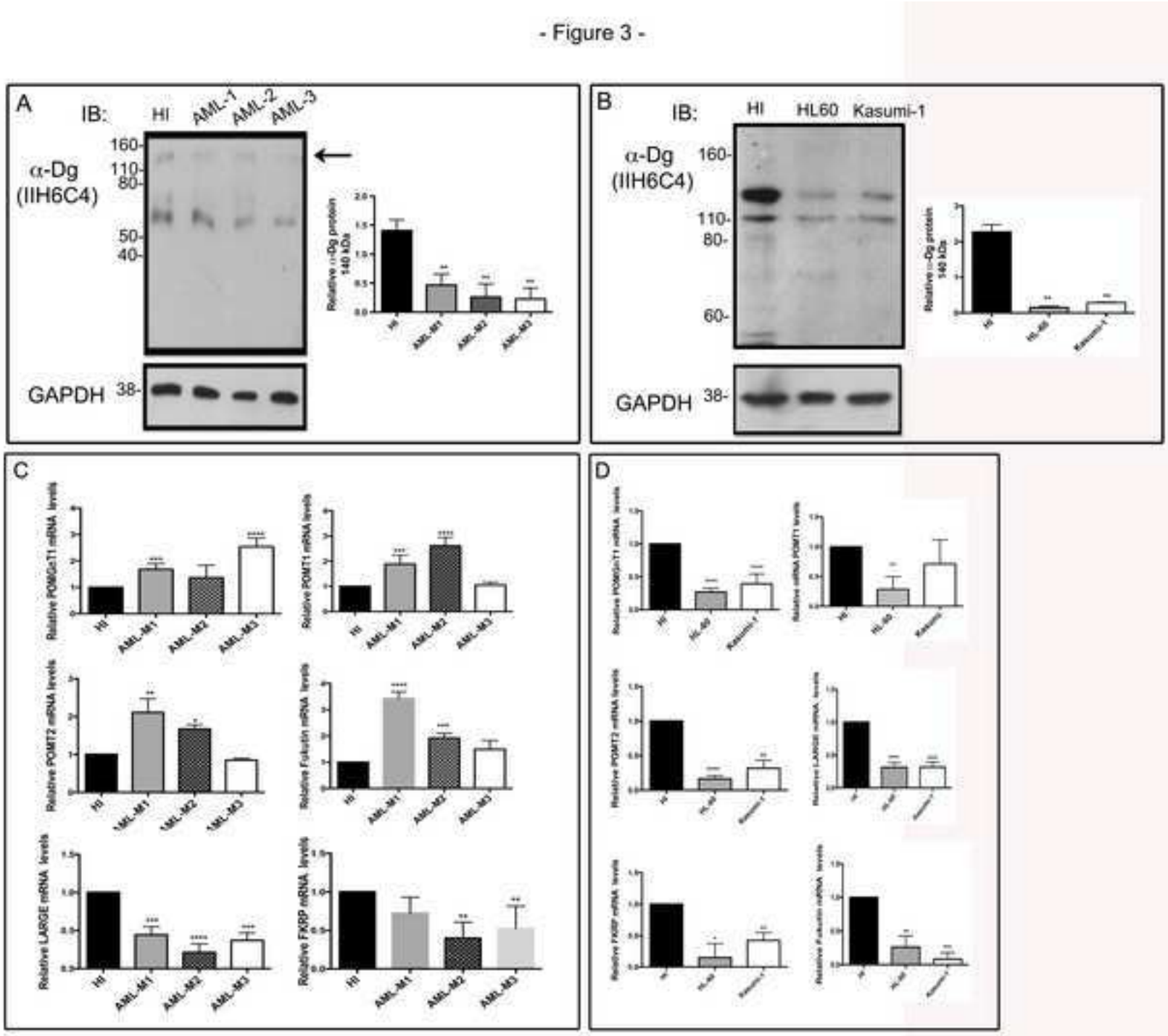

Figure 4

Click here to download high resolution image

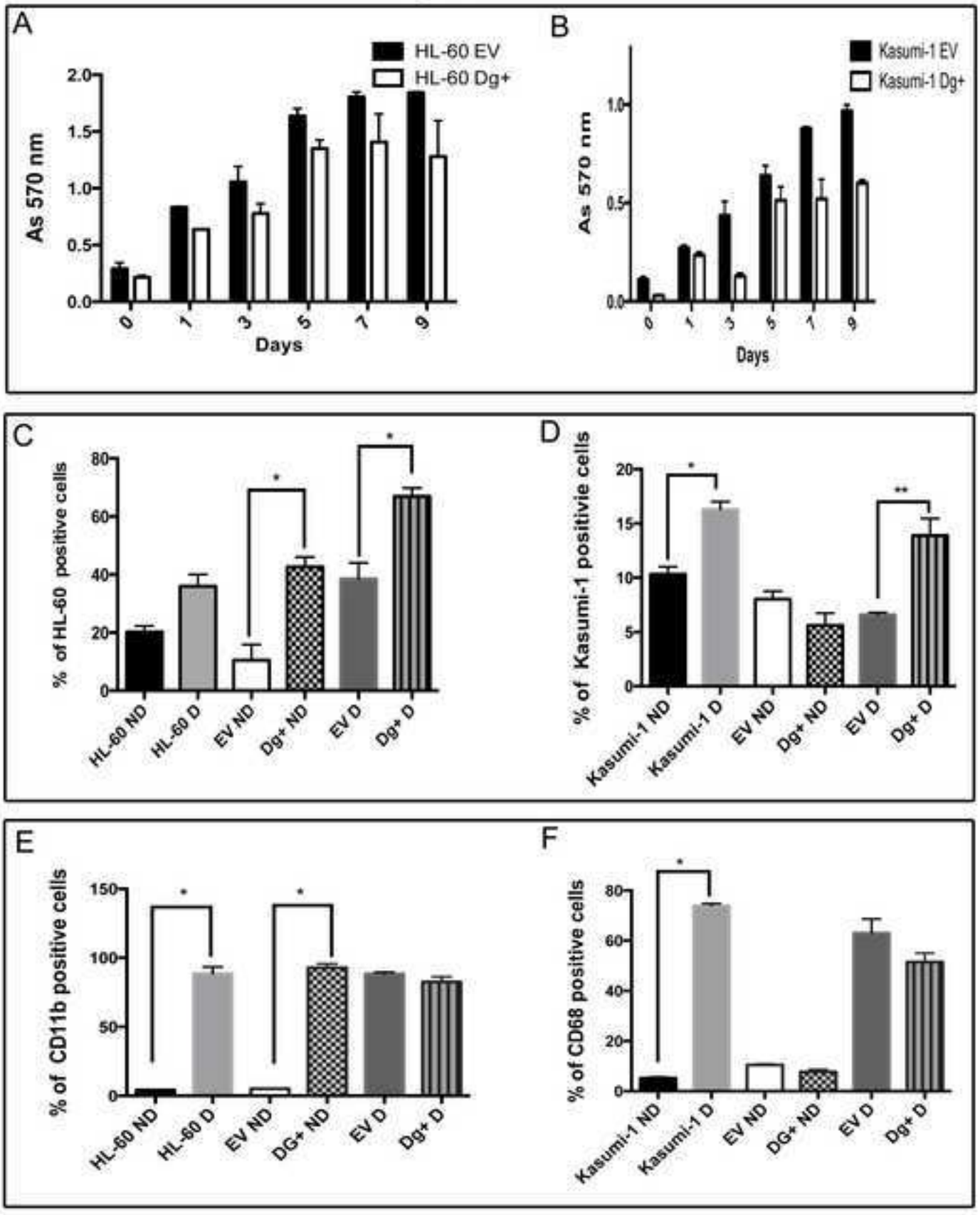

Figure 5

Click here to download high resolution image

- Figure 5 -

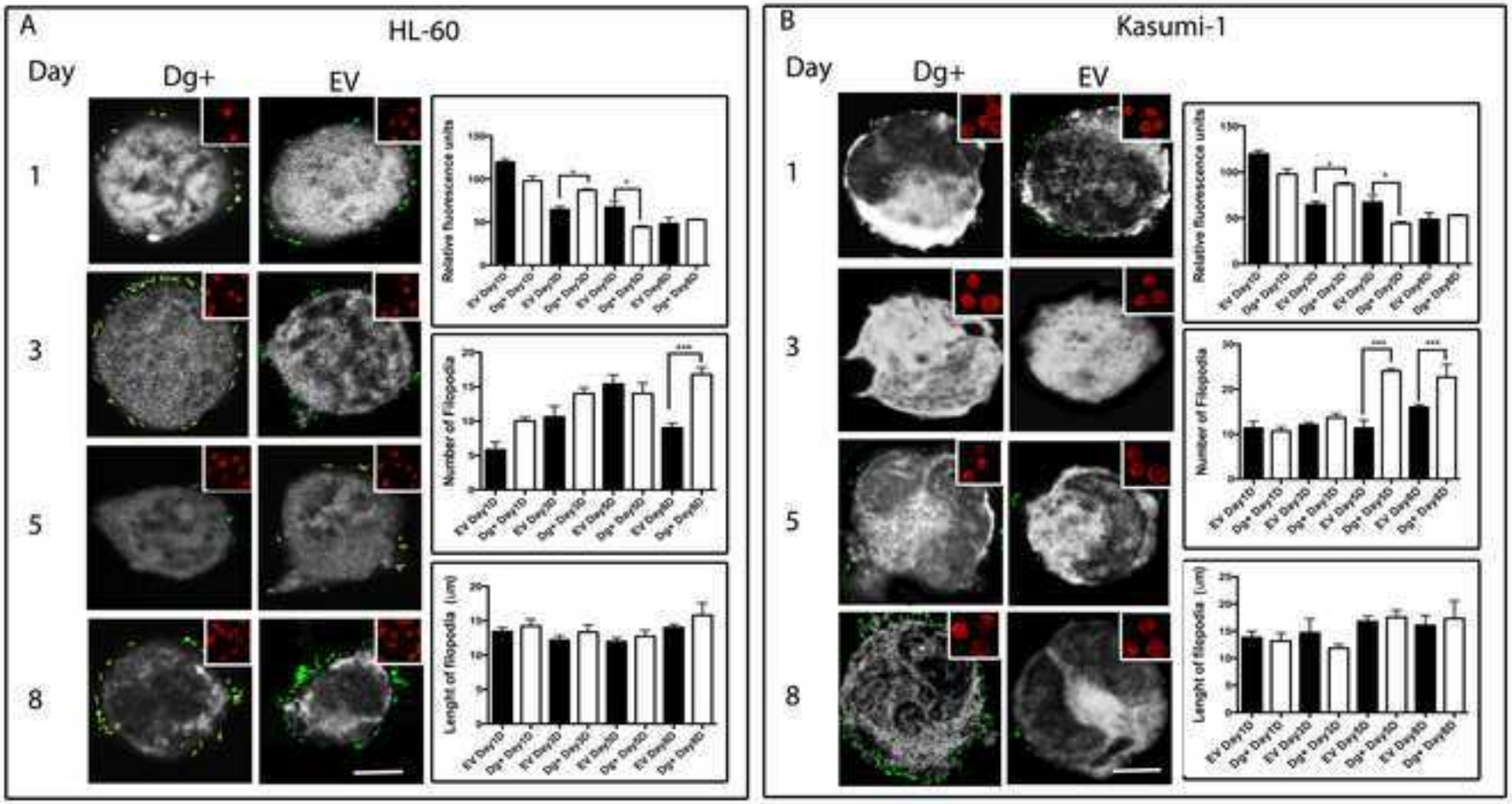

Supplementary Material

Click here to download Supplementary Material: Supplemental Materials and Methods.docx

Table 1

Click here to download Supplementary Material: Table 1.docx

Supplementary Material

Click here to download Supplementary Material: Table 2 s.docx

Supplementary Material

Click here to download Supplementary Material: Supplemetal Figure 1 copia.tif

Supplementary Material

Click here to download Supplementary Material: Supplemental Figure 2.tif